Article:
Gao, H, Wen, D and Sukhorukov, GB (2015) Composite silica nanoparticle/polyelectrolyte microcapsules with reduced permeability and enhanced ultrasound sensitivity. JOURNAL OF MATERIALS CHEMISTRY B, 3 (9). pp. 1888-1897. ISSN 2050-750X

https://doi.org/10.1039/c4tb01717j

Journal of Materials Chemistry B

RSCPublishing

ARTICLE

Composite silica nanoparticle/polyelectrolyte microcapsules with reduced permeability and enhanced ultrasound sensitivity

Cite this: DOI: 10.1039/x0xx00000x

Received 00th January 2014,
Accepted 00th January 2014

DOI: 10.1039/x0xx00000x

www.rsc.org/

Hui Gao,[a] Dongsheng Wen[b] and Gleb B. Sukhorukov[a]

Many chemical and biomedical systems require delivery and controlled release of small molecules, which cannot be achieved by conventional polyelectrolyte-based layer-by-layer capsules. This work proposes an innovative hybrid microcapsule by incorporating in situ formed silica nanoparticles within or on the shell. The influence of various experimental conditions on the stability, mechanical strength and morphology of capsules was investigated, and characterised by SEM, TEM, XRD, EDX and FTIR. The multifunctional capabilities of formed capsules were examined by encapsulating a small molecule Rhodamine B (Rh-B), which could be further released by an ultrasonic trigger. The results show that in situ formed SiO_2 nanoparticles through hydrolysis greatly reduced the permeability of the shell yet with increased mechanical strength and ultrasound response. SiO_2 nanoparticles were shown to be distributed on the surface or inside polyelectrolyte shell, acting as supports for free-standing capsules in both liquid and dry environment. Rapid Rh-B molecules release and the fragmentation of the capsule shells were observed under 50W ultrasound irradiation for a few seconds. Such innovative capsules with capability of small molecule encapsulation and high ultrasound sensitivity could be promising for many applications where pulse release of small molecules is required.

Introduction

Over the past years, there has been increased interest in developing 'smart' micro-/nano-carriers with stimuli-responsive behaviour as effective delivery systems for various applications in pharmaceutics, biotechnology, agriculture, food and cosmetics industries.[1-3] One of the simple but most successful approaches to synthesize microcapsules and to tailor various functions in one entity is the layer-by-layer (LbL) assembly technique, as its step-wise deposition of oppositely charged polyelectrolytes (PEs) facilitates the functionalization of capsule formations.[4-6] However, PE-shelled capsules are difficult to encapsulate cargos with small molecular weights because of the shell's high permeability.[7,8] Increasing shell thickness is a possibility to reduce the permeability, but many layers are required to have a salient change.[9,10] It has been shown that sealing small molecule ($Mw \leq 1000$) was still a challenge even increasing the PE layer number to 18.[11] In addition, an increased shell thickness would increase the difficulty of cargo release. Deposing lipid coatings on the capsules is another way to reduce the shell permeability, but lipids are unstable under high temperature situations, limiting them to only low temperature use.[12] Recently, incorporating inorganic nanoparticles into the organic shell was proposed as an effective method to tune the physical and chemical properties of LbL capsules. By utilizing the merits of both inorganic (nanoparticles) and organic building blocks (shell), such a hybrid approach is promising for making multifunctional capsules suitable for harsh environment. Appropriate engineered, incorporated nanoparticles could increase shell stability and stiffness, reduce shell permeability, and improve capsule's resistance to mechanical and thermal deformation, as well as provide new opportunities for yielding multifunctional microcapsules.[13-16]

In inorganic/PE capsule systems, silica nanoparticles were popularly used as they are water soluble and biocompatible.[15,17,18] The exceptional mechanical properties of silica nanoparticles also make them attractive candidates for functional molecular assemblies.[19-22] Most efforts of design and synthesis of inorganic/organic composite capsules have been focused on assembling prefabricated inorganic nanoparticles into the soft PE multilayer shell.[23-25] This method could produce capsules with relative good control over capsule size, stability and stimuli responsive property, but has considerable challenges in encapsulating and releasing low-molecular-weight molecules (including drugs) from LbL capsules.[26] Instead of using nanoparticles prepared in advance, direct growth of nanoparticles inside or on PEs shells would provide possibilities to decrease the shell porosity, because nanoparticles would nucleate and grow in pores of polymer shells and 'crosslink' with PE multilayers, yielding dense composite shells with a reduced permeability. Sun et al. [15] demonstrated the possibility to grow silica directly on PE surfaces, which were responsible to laser triggering. To prevent

unwanted leakage from loaded capsules, however, many deposition cycles of layered PE-silica coating were required in this procedure, and the capability of encapsulating small molecule (≤ 1000) was not investigated.

Apart from the encapsulation process, controlled release of cargo substance in the predetermined areas is another challenge for any microcapsule delivery system.[27] Different stimuli, such as pH, temperature, laser and microwave radiation, have been investigated to modify the shell permeability and facilitate the release.[28] Such stimuli, however, have limited use in biological and medical systems due to the short penetration depth relating to laser and microwave, and the large side effect associated with changing pH and temperature.[29] In contrast, ultrasound, which is already employed as diagnostics and therapeutic method for many diseases (i.e., prostate cancer), is promising due to its long penetration depth and non-invasive nature.[30] There is, however, very limited investigation on the ultrasonic effect on capsule release.[29,31] It has shown that the shell permeability of capsules embedding with inorganic nanoparticles (i.e., Fe_3O_4 or Au) was very responsive to ultrasound and capsule rupture was observed under high irradiation power (i.e., 100W) for 1-2 minutes.[30,32] However to minimize the damage to healthy tissues, it is important to develop microcapsules with a strong ultrasound sensitivity allowing triggered release, while minimizing the intensity and duration of applied ultrasound.

This work reported an innovative way to fabricate capsules with low permeability yet high ultrasound sensitivity. Without using pre-fabricated nanoparticles, inorganic/PE capsules were made by in situ nucleation and growth of silica nanoparticles inside or on the PE shell surfaces based on the hydrolysis of tetraethyl orthosilicate (TEOS).[15] It is hypothesized that the hydrolysis of TEOS would consume water in polymer shells and form robust SiO_2 during the precipitation process, yielding dense shells with a reduced permeability and adjustable mechanical characteristics. To determine the feasibility of encapsulating small molecule in the resulting silica/PE capsules, Rh-B was used as a typical sample and their controlled release behaviour corresponding to ultrasonic time was studied.

Experimental

Materials

Poly(allylamine hydrochloride) (PAH, Mw= 56000, Sigma), and poly(4-styrenesulfonate) sodium salt (PSS, Mw = 70 kDa, Sigma), fluorescein isothiocyanate (FITC, Mw = 389.38), rhodamine B (Rh-B, Mw = 479), $CaCl_2$, sodium carbonate (Na_2CO_3), ethylenediaminetetraacetic acid (EDTA), tetraethyl orthosilicate (TEOS), NH_4OH and other chemicals were purchased from Sigma-Aldrich. All the chemicals were used as received without further purification.

Composite microcapsule preparation

Polyelectrolyte capsule preparation. Polyelectrolyte microcapsules were assembled via the LbL method on sacrificial calcium carbonate ($CaCO_3$) templates according to Sukhorukov, et al.[33] $CaCO_3$ cores were synthesized freshly by adding 0.33 M Na_2CO_3 solution into the same volume of 0.33M $CaCl_2$ while vigorously stirring. Next, shells were assembled using the as-prepared PAH and PSS solution with a concentration of 2 mg·mL^{-1} in 0.2 M NaCl, depositing 4 PSS/PAH bilayers in total. After that, hollow capsules were obtained by dissolving the core templates in 0.2 M aqueous EDTA. Then they were washed 3 times with pure water (resistivity 18.2 M Ω· cm) and 3 times with ethanol and finally dispersed in ethanol.

Growth of silica. The 2 mL $(PSS/PAH)_4$ capsule suspension in ethanol was diluted into 6 mL. Keeping this solution being magnetic stirred, a certain amount of NH_4OH/H_2O (1:5 in volume) solution and TEOS/ethanol (1:2 in volume) solution were introduced into the capsule suspension. The nucleation and growth of the silica nanoparticles were firstly accelerated at a relatively high temperature (T = 50-60 °C) for different duration time (10-120 minutes). A further growth of silica was allowed to ripen the composite shells at a lower temperature (25 °C) for 20 hours under continuous stirring. Finally the suspensions were centrifuged and washed by ethanol and distilled water for several times.

In-situ dye encapsulation and release.

To examine the feasibility of small molecule encapsulation in formed composite capsules and further quantify their released behaviour under ultrasound irradiation, fluorescent small molecular dye, Rh-B (M w= 479), was chosen as a model cargo substance. Generally, 2 mL fabricated PE microcapsules (containing ~1.25×10^8 capsules) were re-dispersed in 2 mL Rh-B solution (200 μg/mL in ethanol) for 1 hour with stirring. Then the mixture was transferred into a 10 mL beaker, and diluted by 4 mL Rh-B solution. While this suspension was being stirred, 2.5 mL NH_4OH/H_2O (1:5) solution was added firstly, and then 0.1 mL TEOS/ethanol (1:2) solution was dropped slowly (5 minutes for every 0.02 mL), which was heated at 50 °C for 30 minutes then 25 °C for 20 hours. After the growth of silica, capsules were collected and washed several times with ethanol and water to remove free fluorescent substances. The resulting suspension was diluted into 4 mL. Five portions of 200 μL capsule-dye mixtures (containing ~6.25×10^6 capsules) were used for triggered release study (i.e, one portion was kept in dark and another four were treated with ultrasound up to 120 s). After ultrasonication, capsule dye mixture was centrifuged, the supernatant was carefully collected, and the precipitate was added with equal volume of deionized water. Finally, the precipitates were observed by a Leica TS confocal scanning system (Leica, Germany) equipped with a 63×/1.4 oil immersion objective. The fluorescence intensity of each sample (in supernatant) was determined with a fluorescence spectrometer (Perkin-Elmer LS 55) and normalized with the standard fluorescent solutions with known concentrations.

Instrument and Measurement

Ultrasonic treatment was performed by an ultrasonic processor GEX 750 (Sonics & Materials, Inc., USA) operating at 20 kHz, 50W. Scanning electron microscopy (SEM) (FEI Inspect-F) was used to measure the morphologies of dry capsules after gold coating. Samples were observed using an accelerating voltage of 10 kV, a spot size of 3.5, and a working distance of approximately 10 mm. Further morphology and structure of microcapsules as well as the distribution of silica particles were examined by transmission electron microscopy (TEM). Elemental analysis was performed by energy dispersive spectroscopy (EDX) attached to the SEM, and an infrared spectroscopy (FTIR spectrometer 100, Perkin-Elmer) was used to measure the FTIR spectra of vacuum-dried capsule

samples, collecting data at a spectral resolution of 4 cm^{-1}. Confocal laser scanning microscopy (CLSM) images were captured with a Leica TS confocal scanning system (Leica, Germany) equipped with a 63 × /1.4 oil immersion objective.

Results and discussion

Influence of reaction conditions on composite capsule morphology

According to the Stöber reaction, two steps are involved in silica growth process: one is the hydrolysis of TEOS and the other is the condensation of SiO_2 onto the seed surface.[15,34,35]

$$Si(OC_2H_5)_4 + 4H_2O \xrightarrow{NH_3/Alcohol} Si(OH)_4 + 4C_2H_5OH \quad (1)$$

$$Si(OH)_4 \xrightarrow{NH_3/Alcohol} SiO_2\downarrow + 2H_2O \quad (2)$$

Owing to the terminated layer of PAH with amine groups, the surfaces of PE capsules are positively charged which are favored by silicon source (TEOS).[15] Meanwhile, employing ammonia provides the formed silica nanoparticles with a negative, stabilizing surface charge.[35] Therefore, the nucleation and growth of silica directly onto $(PSS/PAH)_4$ PE multilayers via a heterogeneous process is strategically feasible.[15,36] In our practical work, the positively charged capsules should become negatively charged after silica coating, which was demonstrated in this study (Figure S1, Supporting Information). Figure 1 illustrated a schematic process of silica incorporated into PEs microcapsules. After introducing TEOS, NH_4OH and H_2O into the mixture of PE capsules and ethanol, silica would firstly nucleate and deposit inside or on the surface of PE multilayers under appropriate growth environment; Secondly, as SiO_2 particles grow larger, they interact with each other and finally cover the whole shell.

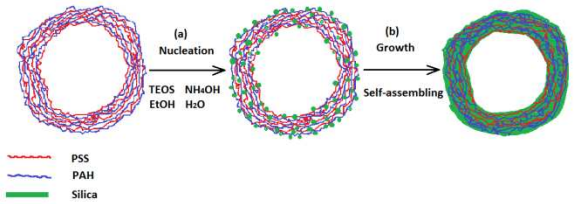

Figure 1 Schematic illustration of $(PSS/PAH)_4$ microcapsule incorporated and strengthened by *in situ* formed silica nanoparticles. (a) silica nucleation and deposition; (b) growth and ripeness process.

In principle, the nucleate and growth rate of inorganic nanoparticles were strongly dependent on the environment such as reaction temperature, time, pH, surfactants, concentration of solutions, etc., so does the formed capsules.[18,37-40] To better control the capsule morphologies, the influence of some key parameters were investigated, as shown in Table 1, and SEM images of the resulting capsule were given in Figure 2.

By fixing the volume ratio of the ammonia to TEOS solution at 25:1, the effects of temperature, solution adding order and holding time on the morphology of the composite

Table 1 Detailed reaction conditions of different samples

	Amount of solution and adding order	Reaction temperature and time
Sample A (S_A)	0 0	0
Sample B (S_B)	0.1 mL TEOS/ethanol, then 2.5 mL NH_4OH/H_2O	25°C-20 h
Sample C (S_C)	0.1 mL TEOS/ethanol, then 2.5 mL NH_4OH/H_2O	60 °C-10 min; 25 °C-20h
Sample D (S_D)	2.5 mL NH_4OH/H_2O, then 0.1 mL TEOS/ethanol	60 °C-10 min; 25 °C-20h
Sample E (S_E)	2.5 mL NH_4OH/H_2O, then 0.1 mL TEOS/ethanol	60 °C-30 min; 25 °C-20h
Sample F (S_F)	2.5 mL NH_4OH/H_2O, then 0.1 mL TEOS/ethanol	50 °C-30 min; 25 °C-20h
Sample G (S_G)	2.5 mL NH_4OH/H_2O, then 0.1 mL TEOS/ethanol	50 °C-120 min; 25 °C-20h
Sample H (S_H)	2.5 mL NH_4OH/H_2O, then 0.5 mL TEOS/ethanol	60 °C-10 min; 25 °C-20h

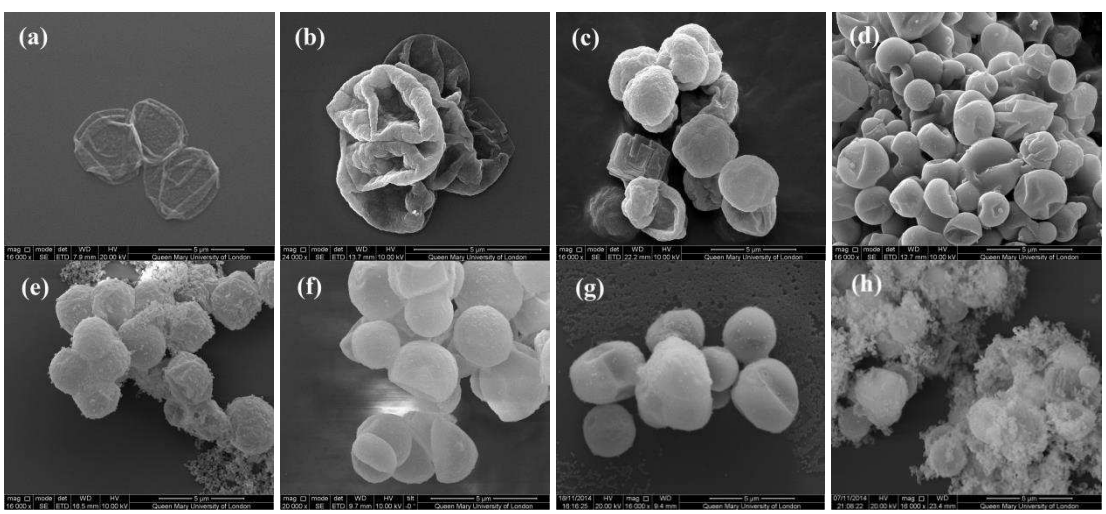

Figure 2 SEM images of composite samples produced by various reaction conditions: (a) sample A; (b) sample B; (c) sample C; (d) sample D; (e) sample E; (f) sample F; (g) sample G; (h) sample H.

microcapsules were studied. Without heat treatment, 0.1 mL TEOS/ethanol solution was firstly introduced into PE capsule suspension, and then 2.5 mL ammonia solution was added dropwise, keeping stirring the mixture at room temperature (25°C) for 20 hours to obtain Sample B (S_B). SEM images indicated that the composite capsules (S_B, Figure 2b) shrunk but were not as flat as those without treating with TEOS (S_A, Figure 2a). A rough surface with many wrinkles and thicker folds were observed, but no spherical shape. S_C was obtained by only changing the reaction temperature to 60 °C for 10 minutes, and the capsules became more robust and most had spherical shape, indicating that the reaction temperature has a great influence on the capsule mechanics. Higher temperature could increase the mobility of reactive components, which therefore facilitates a higher rate of reactivity (hydrolysis, nucleation and growth).[41] It is believed that high temperature accelerated the TEOS hydrolysis rate and promoted the condensation of silica (nucleation), resulting in more silica nanoparticles formed and embedded in the layers. Meanwhile, heat treatment would also affect the morphology of PE capsules due to the (PSS/PAH) shell's sensitivity (shrinkage) to heat.[42] Different to Leporatti et al. [42], who observed that $(PSS/PAH)_5$ microcapsules collapsed in dry state despite of annealing at 70 °C for 2 hours, here we showed that only slight shrinkage of SiO_2-PE capsules was observed after heating at 60 °C for 10-30 minutes.

Comparing Sc, changing the adding order of silicon source and ammonia produced composite capsules (S_D) with a smooth surface, indicating that silica nanoparticles distributed more uniformly on the shell. If ammonia/H_2O solution was firstly added, Figure 2d, the whole system was like an aqueous phase. The subsequently dropped TEOS under fast magnetic stirring was dispersed as droplets in the aqueous phase with abundant ammonia catalyst and H_2O. In this case, TEOS was hydrolyzed very fast according to the hydrolysis reaction equations (1) [43,44] and the partially hydrolysed species were expected to be located on the capsule surfaces.[40] The synthesis would produce the smallest particles due to the initial nucleation of a larger number of particles.[44] Moreover, the presence of ammonia would render the new formed silica particles with a negative surface charge so that those silica particles would be attached to the positive charged PE capsule shells (Figure S1, Supporting Information).[15,35] However, on the contrary, if TEOS was added first, Figure 2c, much rougher shell surface was observed, which may be ascribed to a few reasons: i) TEOS would firstly react with the drops of the newly joined ammonia/H_2O solution and the hydrolysed soluble Si was hardly dispersed uniformly initially due to insufficient amount of H_2O; ii) The initial nucleation number of particles was much less than that of S_D; and iii) The formed negatively charged silica would attach on capsule surfaces during the stirring process and might be slightly aggregated, all these resulting in roughed surfaces.

The effects of duration time were also studied. By prolonging the reaction time at 60 °C to 30 minutes, a more robust structure was obtained as more spherical shaped capsules with lesser folders were appeared in sample E. Their surface became much rougher and a small amount of excessive free silica nanoparticles was found in Figure 2e. The size of the nanoparticles became larger due to a rapid growth of silica under relatively high temperature (60 °C) for a longer period .[44] In order to lower the growth rate of silica particles to avoid this problem, sample F (S_F) was prepared by reducing the reaction temperature to 50 °C but keeping the same duration (i.e., 30 minutes). Figure 2f shows that all capsules possessed smooth surfaces with strengthened free-stranding structure without any breakage. Nanoparticles embedded in their shells distributed homogeneously, and no excess free nanoparticles existed. However, if the duration time at 50 °C was increased to 120 minutes, the composite capsules were still in smooth spherical shape, Figure 2g, but a large number of excessive silica nanoparticles were produced, which is consistent with some early observation.[45] Clearly both temperature and duration time played important roles in controlling the quality of silica coating.

Compared with S_D, i.e., only decreasing the volume ratio of the ammonia to TEOS solution (5:1), Figure 2h showed that large excessive of silica nanoparticles were produced and distributed everywhere. This is, because additional TEOS accelerated the undesired homogeneous nucleation process that produced free silica nanoparticles.[36,46] It was difficult to separate these extra silica nanoparticles from the composite microcapsules. All these results show that the reaction conditions should be controlled carefully to fabricate silica/PEs composite capsules with good qualities. S_F sample was so far the most promising sample and was chosen for further studies, as below.

Element analysis

In order to study whether silica were successfully incorporated, EDX and FTIR were used to analyse the composition of as-prepared hybrid microcapsules. EDX spectrum (Figure 3a) of the composite capsules demonstrated that a large number of C, O, and Si atoms were contained, proving that the capsule wall was built up by the polymer layer and silica. Small amount of Na might come from the original solution, which was not washed out completely. Other small peaks were attributed to

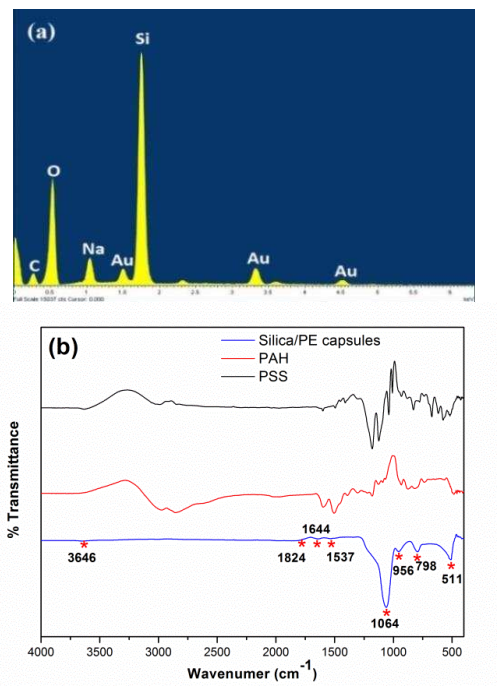

Figure 3 (a) EDX and (b) FTIR spectrums of capsules after silica incorporating (sample S_F).

Au coating. Meanwhile, $CaCO_3$ was all removed by EDTA because no calcium element was found from the spectrum. The FTIR transmittance spectrums of PAH, PSS and composite capsules are shown in Figure 3b. The characteristic bands at 1064, 956 and 798 cm^{-1} were correspond to the stretching, stretching and bending frequencies respectively.[47,48] The position and the shape of the main Si-O vibrational band at 1064 cm^{-1} proved a stoichiometric silicon dioxide structure. Small peak at 956 cm^{-1} belonged to Si-OH stretching and that at 798 cm^{-1} attributed to Si-O bending. Moreover peaks in the spectral range at 511 cm^{-1}, 1537 cm^{-1}, 1644 cm^{-1}, 1824 cm^{-1} and 3646 cm^{-1} were attributed to vibrations of carbon atoms coming from polyelectrolyte part of the composite capsules. Both showed clearly that SiO_2 nanoparticles were successfully incorporated into PE shells.

Morphology and structure analysis

To further investigate the influence of silica incorporation on capsule morphology and their structure, sample F was measured by SEM and transmission electron microscopy (TEM), as given in Figure 4 and Figure 5 respectively. Figure 4 showed that the incorporation of silica nanoparticles in the capsule shell led to significant morphology changes in comparison with nanoparticle-free capsules. Without silica incorporation, all the $(PSS/PAH)_4$ microcapsules were collapsed and flat (Figure 4a and 4c), but on the contrary, the composite microcapsules were structurally reinforced into robust free standing capsules, having three dimensional appearance (Figure 4b and 4d). The external surface consisted of homogeneously distributed SiO_2 nanoparticles embedded in the polyelectrolyte shell, as shown in the Figure 4b and Figure 4d, indicating that the as-made multilayers were sufficiently incorporated by the in situ formed SiO_2 nanoparticles. This was also verified by TEM images. The inset was the SEM image of composite capsules broken by an external force, showing a rough interior surface of the composite shell, which revealed that silica nanoparticles were not only deposited on the exterior surface of the polymeric shell but also being embedded within it and on their interior surfaces. Analysis of SEM (Figure 4) indicated the diameter of dried capsules decreased from ~4.05 µm to ~3.2 µm by coating with silica, but the shell thickness increased a lot, which was further demonstrated by TEM results. Apart from the slight shrinkage of PE layers caused by heat treatment, it is thought that the in situ formation of SiO_2 particles would cross-link and compress the capsule, resulting in a decrease in capsule size yet with an increase in the shell thickness.

Some previous studies reported a problem of limited thickness of the capsule shell even after coating several silica layers.[15,49] However, as shown in Figure 5, the shell thickness increased drastically from a few nanometers to a few hundred nanometers (i.e. ~ 300 nm). The above analysis of SEM images also qualitatively confirmed this. For samples without silica coating, the capsule had relatively smooth surface and in collapsed form, as shown in Figure 5a and Figure 5b, while small dark dots can be found on the surface of composite microcapsules, given in Figure 5c and Figure 5d. Clearly the composite shell became more compact and its permeability should be effectively lowered down due to i) the decrease in capsule size, ii) the increase in shell thickness and iii) a possible increase in the shell density. In particular, benefiting from a better mechanical property of inorganic materials, the incorporation with in situ formed silica nanoparticles would lead to a reinforcement of composite shell mechanics.

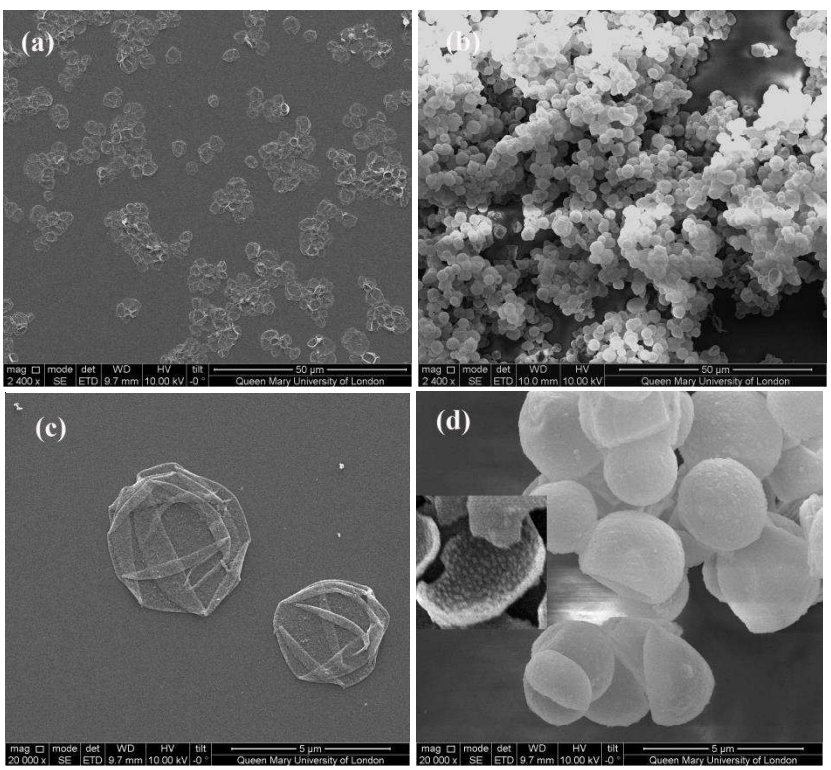

Figure 4 SEM images of $(PSS/PAH)_4$ microcapsules before (a, c) and after (b, d) silica coating (sample S_F).

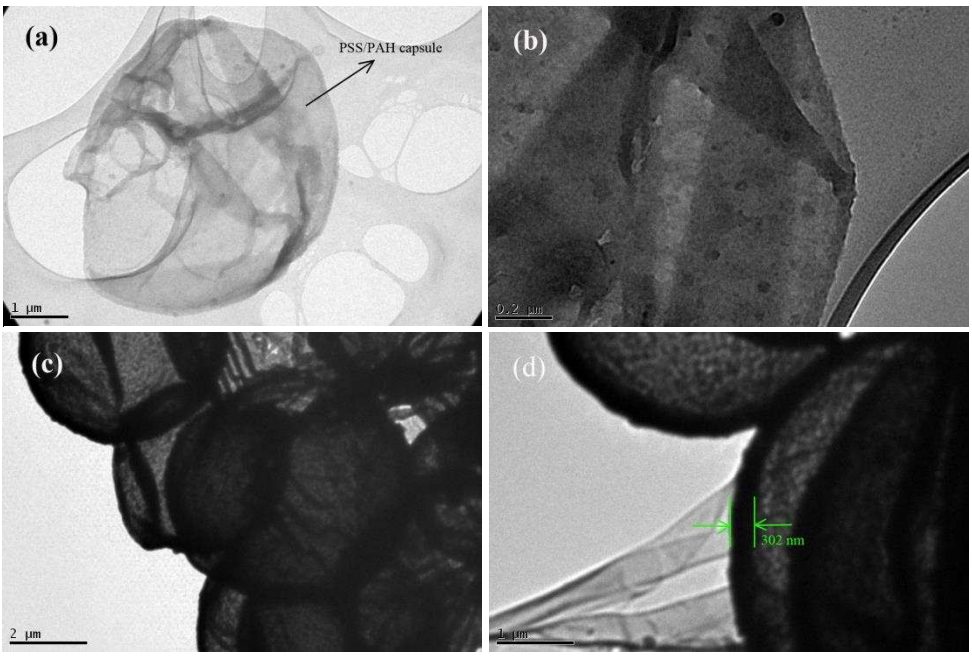

Figure 5 TEM images of capsules without (a, b) and with (c, d) silica coating (sample S_F).

Composite shell reinforcement mechanism and permeability study

During the reaction process, TEOS underwent hydrolysis upon contact with water, according to the net reaction of Eq. (1) and Eq. (2), i.e., $Si(OC_2H_5)_4 + 2H_2O \longrightarrow SiO_2 + 4C_2H_5OH$. This forms solid SiO_2 through a series of condensation reactions catalysed by ammonia and also produces a by-product, ethanol.[50-53] In our study, the hydrolysis and nucleation process were promoted by incubating the mixture at a relatively high temperature (50°C) and a further ripen process was allowed at lower temperature (25°C) for a longer time. A possible incorporation and reinforcement mechanism of the composite structure is illustrated in Figure 1. The pure PSS/PAH multilayer shells were uneven and provided many numbers of nucleation sites. Based on the nucleation principle, new SiO_2 particles would preferably form at the points with low energy, such as at concave points of the shell surfaces, and the pores in polyelectrolyte multilayers.[54] Along with the formation and growth of silica, the polyelectrolyte shell shrunk due to the consumption of water from the multilayer pores as the TEOS was hydrolysed. With prolonging the reaction time (age process), SiO_2 particles would contact and interact with each other and finally cover the whole shell, as illustrated by the TEM results, Figure 5c and Figure 5d. The continuous inorganic nanoparticles would compress the capsule in some degree through the shrinkage process, and the flexible polyelectrolyte layers were restricted. All these factors would result in a decrease in capsule size and an increase in its shell thickness. The pores in capsule shells would become less in amount and smaller in size, and consequently the capsule shell permeability could be drastically reduced, which was further confirmed by CLSM results.

As shown in Figure 6, in sharp contrast to the high permeability of capsules without silica coating (Figure 6a), the polymer shells were condensed by in situ formed SiO_2 nanoparticles and hence the composite capsules performed an effective interception of FITC molecules (Figure 6b). Some composite capsules aggregated together due to the interaction of silica nanoparticles on their surface. The corresponding line scan image demonstrated an average fluorescent signal intensity of ~ 112 units outside the capsules and 0 unit inside the capsules. It is worth mentioning that surface state of capsules would affect the adsorption and transfer of dye molecule.[55,56] To compare the effect of different surface charges on permeability of PE capsule, capsules with PSS as the top layers (negatively charged) were also studied and the result revealed that they were also permeable for the slightly negatively charged FITC molecules (Figure S1 and S2, Supporting Information). Hence, the PSS/PAH capsule permeability for FITC was weakly depended on their surface charge. In some case, surface wettability of capsules could influence their permeability significantly,[56,57] for example, benefitting by hydrophobic property of the capsule shells after UV irradiationYi et al.[57] successfully sealed Rh-B in $(Nafion/DAR)_4$ capsules. Here, as silica nanoparticles are water soluble [15] and our composite capsules were well dispersed in water, the effect of surface wettability could be neglected. Furthermore, the permeability of PE capsules for various molecules decreased to some degree after heat incubation.[42] In order to eliminate the heating effect on the shell permeability for FITC molecules, the pure $(PSS/PAH)_4$ capsules were held at 50 °C for 30 minutes before incubating in the FITC solution. Figure 6a demonstrated that PSS/PAH capsules were still permeable for FITC, which is consistent with the early observation that PE capsule was not sufficient to encapsulate small fluorescein molecules by heat treatment only.[58] Moreover, with a detailed look at the intact composite shells in Figure 6b, bright green rings were not found, which implied that FITC molecules were prevented to go into the shells. These results again confirmed that the permeability of microcapsules was reduced significantly after silica incorporation, consistent with SEM and TEM results and the hypothesis of capsules sealing by in situ formed nanoparticles.

Ultrasound responsive properties

Remote activation of microcapsules was conducted using an ultrasonic setup operating at a frequency of 20 kHz and power output 50 W. The suspension of microcapsules was submitted to ultrasound sonication for different duration times (2, 4, and 6 s). A high ultrasonic sensitivity of the composite microcapsules was evidenced. Figure 7 shows the resulting SEM images of capsules with different shell composition stimulated for different ultrasound duration time. It is clearly seen that pure $(PSS/PAH)_4$ capsules were slightly deformed after sonication, whereas the silica–composite capsules were broken into small fragments. Such an observation is consistent with several other reports, which showed that the ultrasound sensitivity of the PSS/PAH capsules could be remarkably increased if nanoparticles were embedded in the polyelectrolyte network.[23,32] Most of composite capsules were broken after only 2s' sonication. From the broken fragments, it shows clearly that the shell thickness of the fragments decreased with increasing sonication time, because more silica nanoparticles were separated from the composite shells. For 6s' ultrasonication, the fragments became much smaller with a large portion of small dots appearing. One reasonable explanation for the increased sensitivity is that the incorporation of SiO_2 nanoparticles increased the density gradient across the water/shell interface and consequently improved the absorption of acoustic energy.[29] Another possible explanation is the modification of the shell's

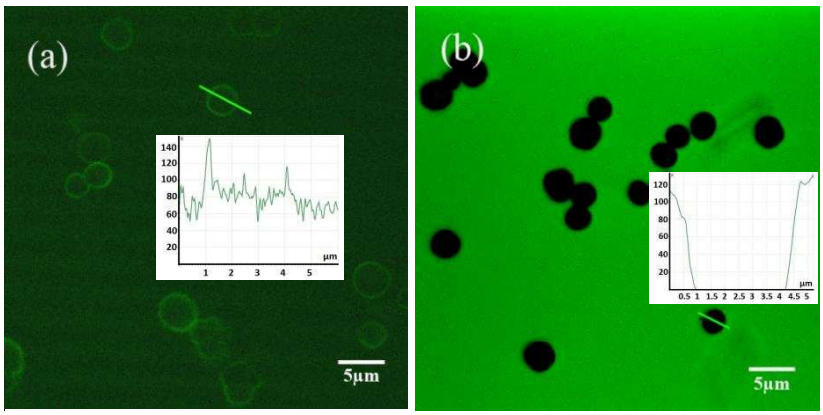

Figure 6 CLMS images of microcapsules without and with silica incorporation dispersed in FITC solution. (a) pure $(PSS/PAH)_4$ after held at 50 ºC for 30 minutes, (b) $SiO_2/(PSS/PAH)_4$ composite capsules. The line scan insets showed relative fluorescent intensity in the corresponding capsules.

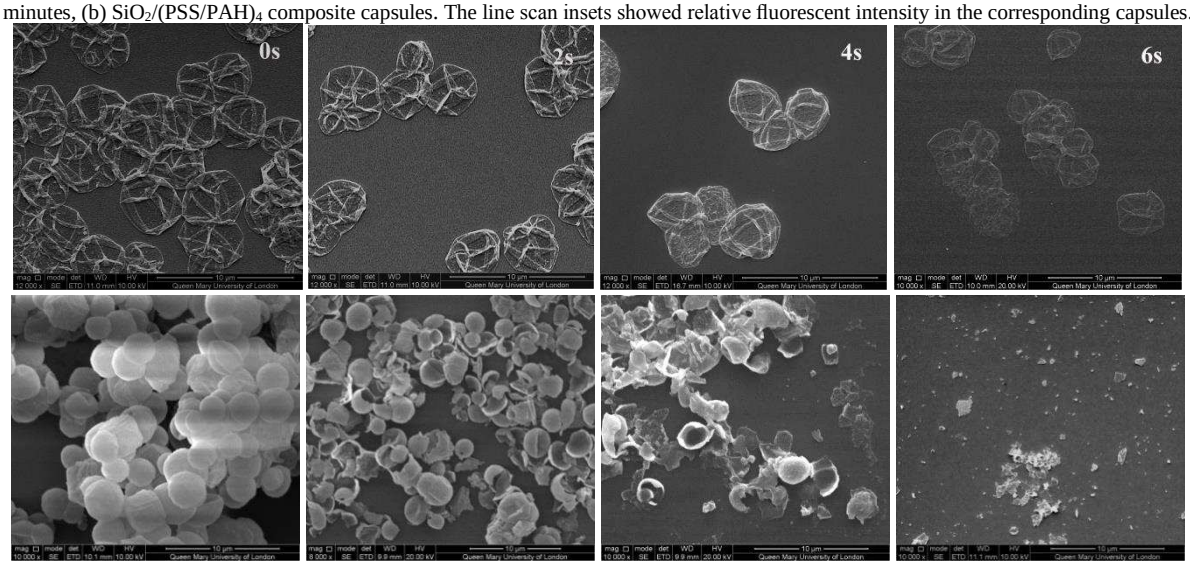

Figure 7 SEM images of pure capsules (top) and composite capsules (bottom) response to ultrasound with respect to the sonication time.

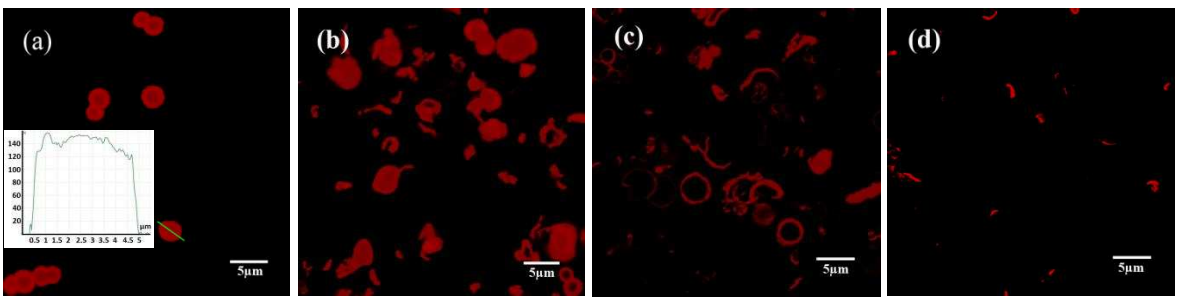

Figure 8 CLSM images of Rh-B containing composite microcapsules after ultrasound treatment with different time: (a) 0s; (b) 2s; (c) 4s; (d) 6s. The free Rh-B was removed by washing for several times before the measurement. Line scan inset showed relative fluorescent intensity in the corresponding capsules.

mechanical properties. It was known that the concentration of nanoparticles in the capsule shell could affect the capsule stability.[30] As the concentration reached to a critical point, the nanoparticle interaction effect increased, exceeding the effect of the polyelectrolyte matrix, and played a major role in the shell mechanics.[13] In addition, embedding inorganic nanoparticles in the microcapsule shell could increase the shell stiffness significantly.[14,59] Clearly the presence of rigid nanoparticles within soft polymeric shells reduced the shell elasticity, which made them prone to break during ultrasonic treatment with different fracture patterns.

Mass encapsulation and release triggered by ultrasound

With a reduced permeability and strong ultrasound sensitivity, silica/polyelectrolyte composite capsules should be promising for small molecule encapsulation and controlled release by ultrasound. Rh-B was chosen as a cargo material instead of FITC due to its longer life time. It is expected that the formation and growth of silica nanoparticle within polymer multilayers and on their internal and outside surfaces provided adequate capability to seal the shells and therefore to entrap Rh-B. Before the ultrasound treatment, a strong fluorescent signal (i.e., over 150 units in intensity) was detected, Figure 8a. Further ultrasound treatment caused a rapid release of capsule ingredients (Figure 8b-d). After 6s of ultrasound irradiation, only very small debris with limited fluorescent signal can be observed (Figure 8d).

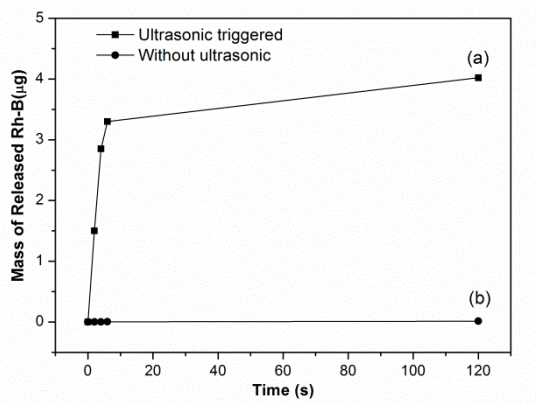

Figure 9 Mass of released Rh-B from composite capsules. (a) ultrasonic triggered release; (b) without any treatment.

Quantitative measurement of the dye release characteristics (i.e., a combined effect of diffusion and ultrasound effect) was shown in Figure 9a. It was estimated that the total mass of the encapsulated Rh-B was 5.0 μg inside ~6.25×10^6 capsules in this work (i.e., ~ 0.8 pg per capsule). As shown in Figure 9a, the released Rh-B increased rapidly following the ultrasound triggering. ~30% of the fluorescent dyes was released in just 2s, and it increased to 66% in 6 s. The release curve became flatted after that, reaching a value of ~80% after 120s. In contrast, without ultrasound triggering, the encapsulated Rh-B released very slowly (Figure 9b), only ~0.26% of the encapsulated dyes was detected after 120s. If prolonging the time to 1 hour, the value reached to 7.6% and two days later, 43% of the dyes were diffused outside the capsules (Figure S3, Supporting Information). Obviously, ultrasonic stimulation is an effective and efficient way to release the encapsulated compounds in silica/PE capsules. It should be noted here that not all the encapsulated dyes were released (as detected). Besides the possible photobleaching effect, some fluorescent dyes were adsorbed on composite capsule shells, as shown in CLSM images (Figure 8b-d).

For ultrasound with high power of 50 W, a few seconds is enough to break the silica/PE capsules and let the cargo be released. On the contrary, a relative long duration time is needed to damage the composite shells if the ultrasound power is low, for example, ultrasound for medical use (1 MHz, 1-5W).[30] Destruction behaviours of the composite capsules induced by low power ultrasound in a more gentle way will be further studied. It is believed that the proposed idea in this work, i.e., novel composite capsules with the capability of small molecule encapsulation and their rapid release triggered by ultrasound, could be extended to many medical applications, which warrants its future investigations.

Conclusions

In summary, we proposed and confirmed a new nanoparticle-reinforced composite microcapsule system that has low permeability, high mechanical strength and strong ultrasound sensitivity. Silica nanoparticles were successfully introduced into prefabricated LbL PE microcapsules by in situ hydrolysis of TEOS. The hydrolysis consumed water in polymer shells and formed robust SiO_2 during the precipitation process, yielding dense shells with a reduced permeability. The morphology and mechanical properties of composite capsules were found to be tuneable by adjusting several parameters such as temperature, holding time, adding order and the amount of TEOS. SiO_2 nanoparticles were shown to be distributed on the surfaces or inside polyelectrolyte shell, acting as supports for free-standing capsules in both liquid and dry environment. CLSM study confirmed that the permeability of the composite capsules was reduced significantly. As an example study, the composite capsules were successfully used to encapsulate a small molecule cargo, Rh-B. Further exposure of these capsules to ultrasound treatment showed an irreversible shell rapture and rapid cargo release in a few seconds. Such innovative multifunctional capsules are promising for many future applications including controlled drug delivery and release.

Acknowledgements

Authors would like to thank Dr Zofia Luklinska, Mr Russell Bailey and Dr Dongsheng Wu for assistant in SEM, TEM and LSCM measurements. Authors thank Professor Yuri Gunko (Trinity College Dublin) for stimulating discussions. H.G. thanks financial support from China Scholarship Council for her Ph.D. study.

Notes and references

[a] The School of Engineering and Materials Science, Queen Mary, University of London, Mile End Road, London, E1 4NS, Tel: +44 (0)20 7882 5508; Email: g.sukhorukov@qmul.ac.uk
[b] Institute of Particle Science and Engineering, University of Leeds, Leeds, LS2 9JT; Tel: 0113 3431299; Email: d.wen@leeds.ac.uk

1 Y. Ma, W. Dong, M. A. Hempenius, H. MÖhwald and G. Julius Vancso. Angew. Chem. Int. Ed., 2007, **46**, 1702 – 1705.

2 B. G. Stubbe, K. Gevaert, S. Derveaux, K. Braeckmans, B. G. De Geest, M. Goethals, J. Vandekerckhove, J. Demeester and S. C. De Smedt, Adv. Funct. Mater., 2008, **18**, 1624 – 1631.

3 D. Sen, J. Bahadur, S. Mazumder, G. Verma, P. A. Hassan, S. Bhattacharya, K. Vijai and P. Doshi. Soft Matter, 2012, **8**, 1955 – 1963.

4 M. A. C. Stuart, W. T. S. Huck, J. Genzer, M. MÜller, C. Ober, M. Stamm, G. B. Sukhorukov, I. Szleifer, V. V. Tsukruk, M. Urban, F. Winnik, S. Zauscher, I. Luzinov and S. Minko, Nat. Mater., 2010, **9**, 101 – 113.

5 R. Klitzing, Phys. Chem. Chem. Phys., 2006, **8**, 5012 – 5033.

6 E. Donath, G.B. Sukhorukov, F. Caruso, S.A. Davis and H. Möhwald. Angew. Chemi. Int. Ed., 1998, 37, 2202– 2205.

7 V. Kozlovskaya, E. Kharlampieva, M.L. Mansfield and S. A. Sukhishvili, Chem. Mater., 2006, **18**, 328 – 336.

8 Q. Yi and G. B. Sukhorukov. Part. Part. Syst. Charact., 2013, **30**, 989 – 995.

9 E. Blomberg, E. Poptoshev, P. M. Claesson and F. Caruso. Langmuir, 2004, **20**, 5432 – 5438.

10 G. B. Sukhorukov, E. Donath, S. A. Davis, H. Lichtechfeld, F. Caruso, V. I. Popov and H MÖhwald. Polym. Adv. Technol., 1998, 9, 759 – 767.

11 W. F. Dong, K. Ferri James, A.Thorsteinn, S. Monika, G. B. Sukhorukov and H MÖhwald. Chem. Mater., 2005, **17**, 2603 – 2611.

12 S. Moya, E. Donath, G. B. Sukhorukov, M. Auch, H. Baumler, H. Lichtenfeld and H MÖhwald. Macromol., 2000, **33**, 4538 – 4544.

13 M. F. Bedard, A. Munoz-Javier, R. Mueller and P. Pino. Soft Matter, 2009, **5**, 148 – 155.

14 X. Liang, B. Xu, S. Kuang, and X. Wang. Adv. Mater., 2008, **20**, 3739 – 3744.

15 B. Sun, S. A. Mutch, R. M. Lorenz, and D. T. Chiu. Langmuir, 2005, **21**, 10763 – 10769.

16 S. A. McCarthy, G. L. Davies and Y. K. Gun'ko. Nat. protoc., 2012, 7, 1677–1693.

17 S. H. Wu, Y. Hung and C. Y. Mou. Chem. Commun., 2011, 47, 9972–9985.

18 G. L. Davies, A. Barry and Y. K. Gun'ko. Chem. Phys. Lett., 2009, 486, 239–244.

19 P. Erni, G. Dardelle, M. Sillick, K. Wong, P. Beaussoubre, and W. Fieber. Angew. Chem. Int. Ed., 2013, **52**, 10334 –10338.

20 Y. Yang, Z. Wei, C. Wang, and Z. Tong. ACS Appl. Mater. Interfaces, 2013, **5,** 2495 – 2502.

21 Z. Niu, Z. Yang, Z. Hu, Y. Lu and C. C. Han. Adv. Funct. Mater., 2003, **13**, 949 – 954.

22 J. Li, Z. Jiang, H. Wu, L. Zhang, L. Long and Y. Jiang. Soft Matter, 2010, **6**, 542 – 550.

23 M. N. Antipina and G. B. Sukhorukov. Adv. Drug Deliv. Rev., 2011, **63**, 716 – 729.

24 K. Zhang, W. Wu, K. Guo, J. F. Chen and P. Y. Zhang. Langmuir, 2010, **26**, 7971 – 7980.

25 K. Zhang, Q. Wang, H. Meng, W. Wu and J. Cheng. Particuology, 2014, **14**, 12 – 18.

26 P. R. Gil, L. L. del Mercato, P. del Pino, A. Muñoz Javier, and W. J. Parak. Nano Today, 2008, **3**, 12 – 21.

27 Q. Yi and G.B. Sukhorukov. ACSNANO, 2013, **7**. 8693 – 8705.

28 M. Delcea, H. Möhwald and A.G. Skirtach. Adv. Drug Deliv. Rev., 2011, **63**, 730 – 747.

29 T. A. Kolesnikova, D. A. Gorin, P. Fernandes, S. Kessel, G. B. Khomutov, A. Fery, D. G. Shchukin, and H. Möhwald. Adv. Funct. Mater., 2010, **20**, 1189 – 1195.

30 D. G. Shchukin, D. A. Gorin, and H. Möhwald. Langmuir, 2006, 22, 7400 – 7404.

31 D. Lensen, E. C. Gelderblom, D. M. Vriezema, P. Marmottant, N. Verdonschot, M. Versluis, N. de Jong and J. C. M. van Hest. Soft Matter, 2011, **7**, 5417 – 5422.

32 A. G. Skirtach, B. G. De Geest, A. A. Mamedov, A. A. Antipov, N. A. Kotov and G. B. Sukhorukov, J. Mater. Chem., 2007, **17**, 1050 – 1054.

33 G. B. Sukhorukov, E. Donath, H. Lichtenfeld, E. Knippel, M. Knippel, A. Budde and H. MÖhwald, Colloids Surf., A: Physicochem. Eng. Aspects, 1998, **137**, 253 – 266.

34 S. C. Warren, M. R. Perkins, A. M. Adams, M.Kamperman, A. A. Burns, H. Arora, E. Herz, T. Suteewong, H. Sai, Z. H. Li, J. Werner, J. Song, U. Werner-Zwanziger, J. W. Zwanziger, M. Grätzel, F. J. DiSalvo and U. Wiesner. Nat. Mater., 2012, **11**, 460 – 467.

35 A. van Blaaderen, J. van Geest and A .Vrij. J. Colloid Interface Sci., 1992, **154**, 481 – 501.

36 Y. Yin, Y. Lu, Y. Sun and Y. Xia. Nano. Lett., 2002, **2**, 427 – 430.

37 B. R. Li, H. Gao, Y. Q. Guo and S. X. Hou. Cryst. Eng. Comm., 2012, **14**, 4168 – 4172.

38 A. S. Myerson and B. L. Trout. Sci., 2013, **23**, 855 – 856.

39 D. L. Green, J. S. Lin, Y. F. Lam, M. Z. C. Hu, D. W. Schaefer, and M. T. Harris. J. Colloid Interface Sci., 2003. **266**, 346 – 358.

40 F. J. Arriagada and K. Osseo-Asare. Colloids and Surfaces A: Physicochem. Eng. Aspects, 1999, **154**, 311 – 326.

41 B. R. Li, H. Gao, J. J. Liu and Z. W. Yang. J. Cryst. Growth, 2012, **351**, 169 – 175.

42 S. Leporatti, C. Gao, A. Voigt, E. Donath and H. Möhwald. Eur. Phys. J. E., 2001, **5**, 13 – 20.

43 S. Fouilloux, O. Tache, O. Spalla, and A. Thill. Langmuir, 2011, **27**, 12304 – 12311.

44 T. Yokoi, J. Wakabayashi, O. Yuki, F. Wei, M. Iwanma, R. Watanabe, L. Aramaki, A. Shimojima, T. Tatsumi and Y. Okubo. Chem. Mater., 2009, **21**, 3719 – 3729.

45 D. J. Tobler and L. G. Benning. Cosmochimica Acta, 2013, **114**, 156 – 168.

46 V. V. Hardikar and E. J. Matijeviæ. Colloid Interface Sci., 2000, **221**, 133 – 136.

47 S. Musić, N. Filipović-Vinceković and L. Sekovanić. Brazilian J. Chem. Eng., 2011, **28**, 89 – 94.

48 J. P. Bange, L. S. Patil, and D. K. Gautam. Prog. Electromagn. Res. M., 2008, **3**, 165 – 175.

49 Y. Kobayashi, K. Misawa, M. Kobayashi, M. Takeda, M. Konno, M. Satake, Y. Kawazoe, N. Ohuchi and A. Kasuya. Langmuir, 2004, 242, 47 – 52.

50 X. Deng, L. Mammen, Y. F. Zhao, P. Lellig, K. Müllen, C. Li, H. J. Butt, and D. Vollmer. Adv. Mater., 2011, 23, 2962 – 2965.

51 M. Frampton, A. Vawda, J. Fletcher and P. M. Zelisko. Chem. Commun., 2008, 5544 – 5546.

52 T. Suteewong, H. Sai, R. Hovden, D. Muller, M. S. Bradbury, S. M. Gruner and U. Wiesner. Sci., 2013, 340, 337 – 412.

53 S. H. Zhi, J. Xu, R. Deng, L. S. Wan and Z. K. Xu. Polym., 2014, 55, 1333 – 1340.

54 J. J. De Yoreo and P. G. Vekilov. Rev. Mineral. Geochem., 2003, 54, 57 – 93.
55 T. Lu, Z. Wang, Y. Ma, Y. Zhang and T. Chen. Int J Nanomedicine. 2012, 7, 4917 – 4926.
56 W. C. Mak, J. Bai, X. Y. Chang and D. Trau. Langmuir, 2009, 25, 769 – 775.
57 Q. Yi and G. B. Sukhorukov. ACS Appl. Mater. Interfaces, 2013, 5, 6723 – 6731.
58 K. Köhler and G. B. Sukhorukov. Adv. Funct. Mater., 2007, 17, 2053 – 2061.
59 A. M. Pavlov, V. Saez, A. Cobley, J. Graves, G. B. Sukhorukov and T. J. Mason. Soft Mater, 2011, 7, 4341 – 4347.

